VLT/UVES Observations of IS Molecules and DIBs in the Magellanic Clouds

D. Welty (Chicago), S. Federman (Toledo), R. Gredel (MPIfA), D. Lambert (Texas), and J. Thorburn (Chicago)

Abstract

We discuss the abundances of interstellar CH, CH^+, and CN in the Magellanic Clouds, derived from high S/N spectra of 5 SMC and 12 LMC stars obtained with the VLT/UVES. We detect CH and/or CH^+ toward 2 SMC and 8 LMC stars, and detect CN toward the LMC star Sk−67°2. To our knowledge, these are the first reported detections of these molecular species in the ISM of the Magellanic Clouds, apart from those of CH and CH^+ toward SN 1987A. The column densities now available for CH, H_2, K I, and Na I indicate that all four species are typically less abundant (relative to H I) in the Magellanic Clouds than in our Galaxy, presumably due to the lower metallicities and generally stronger ambient radiation fields there. The relationships among those four species, however, appear to be similar to the ones observed in the Galactic ISM, except that Na I/H_2, K I/H_2, and CH/H_2 are generally lower in the SMC.

Toward most of our targets, the UVES spectra also reveal absorption at SMC or LMC velocities from several of the typically strongest of the enigmatic diffuse interstellar bands (e.g., those at 5780, 5797, and 6284 Å). Several of the so-called "C_2-DIBs", associated with enhanced C_2 and CN, are also detected toward Sk−67°2. In most cases, the Magellanic Clouds DIBs are weaker, for a given N(H), than those typically observed in our Galaxy (again presumably due to the lower metallicities and stronger radiation fields) — but they are also weaker, relative to $E(B-V)$, Na I, and K I, than in the Milky Way.

Introduction

Studies of the interstellar medium (ISM) in the Magellanic Clouds (MC) explore somewhat different environmental conditions from those typically probed in our own Galactic ISM. The MC are characterized by lower overall metallicities (−0.3 dex for the LMC, −0.6 to −0.7 dex for the SMC), lower dust-to-gas ratios, generally stronger ambient radiation fields, and significant differences in UV extinction (especially in the SMC). These differences are predicted to affect the structure and properties of interstellar clouds in the LMC and SMC (Wolfire et al. 1995; Pak et al. 1998) and, in principle, they may also affect the relative abundances of various constituents of those clouds. Comparisons of the relative interstellar abundances of atomic and molecular species — for the different environments in the Milky Way, the LMC, and the SMC — may thus give insights into the physical and chemical processes shaping the clouds. In addition, observations of the diffuse interstellar bands — thought to be due to large, carbon-based molecules — in the Magellanic Clouds may yield useful constraints on the DIB carriers.

Unfortunately, very little is known regarding optical/UV absorption from molecules in the Magellanic Clouds, apart from the recent *FUSE* H_2 survey of Tumlinson et al. (2002). We have therefore obtained high S/N, moderately high resolution optical spectra of a number of stars in the LMC and SMC, in an attempt to expand the sample of detections of CH, CH^+, CN, and DIBs — so that we may then compare the relative abundances of those species with the values and trends found in our Galaxy.

VLT/UVES Spectra of SMC and LMC Stars

Seventeen Magellanic Clouds sightlines (5 SMC, 12 LMC) are included in this mini-survey. As most of the sightlines were selected for having strong observed absorption from H_2 (Tumlinson et al. 2002) and/or Na I (Welty 2005), it is not an unbiased sample. The targets have V magnitudes between 10.9 and 13.8 and Magellanic Clouds color excesses ranging from 0.07–0.18 mag (SMC) and from 0.08–0.51 mag (LMC) (after subtracting Galactic foreground contributions).

Spectra of the targets were obtained with the ESO/VLT UT2 telescope and UVES spectrograph, under several different observing programs executed in 2002–2004. Most were observed using the standard dichroic 1 390/564 setting and a slit width corresponding to 0.7 arcsec — yielding nearly complete coverage of the wavelength range from 3260 to 6680 Å at a resolution of 4.5–4.9 km s^{-1}. This setup includes lines from Na I (U and D doublets), Ca I, Ca II, and Ti II; the strongest lines from CH, CH^+, and CN; and a number of the diffuse interstellar bands. Standard routines within IRAF were used to obtain extracted, wavelength-calibrated spectra from the raw CCD frames. The empirical S/N ratios in the summed, normalized UVES spectra are typically ∼ 200–350 per half resolution element near the various molecular lines.

Some of the normalized CH^+ λ4232 and CH λ4300 profiles are displayed together with the corresponding Na I λ5895 profiles in Figure 1; the CH^+, CH, CN λ3874, and Na I λ3302 profiles observed toward the LMC star Sk−67°2 are shown in Figure 2. In most cases, the molecular lines lie at the same velocity as the strongest Na I absorption. The higher resolution (FWHM ∼ 1.2–2.0 km s^{-1}) Na I λ5895 spectra (Welty 2005) reveal both more complex structure than the UVES spectra and additional lower column density components — suggesting that some of the molecular absorption features may be unresolved blends of several narrower components.

CH and/or CH^+ are detected with greater than 2-σ significance toward many of the LMC stars, but only toward one star (AV476) in the SMC. Typical (detected) equivalent widths for the CH λ4300 line and for the CH^+ λ4232 line are both ∼ 1–5 mÅ; 3-σ limits for weak, unresolved lines are generally ∼ 1.2–1.8 mÅ. Even at such fairly sensitive limits — and for sightlines generally selected for having relatively strong absorption from H_2 and/or Na I — CN is detected only toward the LMC star Sk−67°2, at 4.9±0.4 mÅ for the B-X (0,0) R(0) line at 3874.6 Å. To our knowledge, these are the first reported detections of these molecules in the ISM of the Magellanic Clouds, apart from CH λ4300 (0.9±0.2 mÅ) and CH^+ λ4232 (0.4±0.2 mÅ) toward SN 1987A (Magain & Gillet 1987).

The diffuse interstellar bands at 5780, 5797, and 6284 Å are typically among the strongest and most frequently observed DIBs in the Galactic ISM. Figures 3 and 4 show the absorption from the DIBs at 5780 and 5797 Å toward some of the SMC and LMC targets, respectively. For all three of these DIBs, weak, broad absorption features — centered at velocities similar to those of the strongest Magellanic Clouds Na I components and with central depths generally ≲ 2% below the local continuum — appear to be present toward nearly all of the SMC and LMC targets. The equivalent widths for the Magellanic Clouds DIBs range from 14 to 111 mÅ for the 5780 Å DIB and from 4 to 23 mÅ for the 5797 Å DIB, with uncertainties ∼ 2–10 mÅ. The equivalent widths for the broader 6284 Å DIB range from about 50 to 180 mÅ, with uncertainties ∼ 20 mÅ. The three DIBs generally are weaker than those measured toward several more reddened stars by Ehrenfreund et al (2002), and are more similar in strength to those seen toward SN 1987A [$E(B-V)$ = 0.10 mag; Vidal-Madjar et al. 1987].

Column Densities

Because the molecular lines observed toward these Magellanic Clouds targets are weak, fairly accurate total column densities may be obtained directly from the equivalent widths (assuming the lines to be optically thin), by integrating the "apparent" optical depth over the line profiles, and/or via multi-component fits to the line profiles. In the Galactic ISM, even fairly strong DIBs appear to be unsaturated (Thorburn et al. 2003) — so the column densities of the DIB carrier(s) are assumed to be proportional to the corresponding equivalent widths.

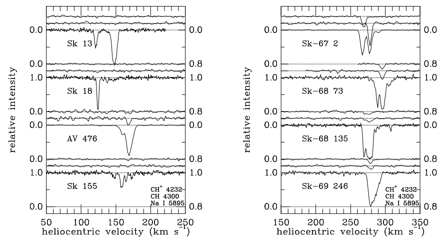

Figure 1. Absorption lines of CH^+ (λ4232), CH (λ4300), and Na I (λ5895) toward 4 SMC (*left*) and 4 LMC (*right*) stars. Only the Magellanic Clouds absorption is shown. The CH^+ and CH spectra are from the VLT/UVES (FWHM = 4.5 km s^{-1}); most of the Na I spectra are from the ESO/3.6m/CES (FWHM = 1.2-2.0 km s^{-1}). The vertical scale is expanded by a factor of 5 for the molecular lines (*right-hand scales*).

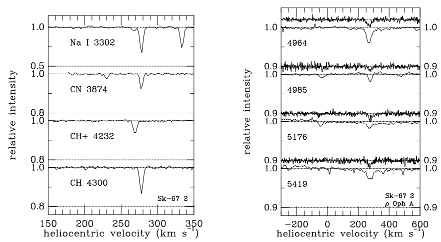

Figure 2. (*left*) Absorption lines of Na I, CN, CH^+, and CH toward the LMC star Sk−67°2. Only the LMC absorption is shown. The vertical scale is expanded by a factor of 5 for the molecular lines. The weaker member of the Na I λ3302 doublet appears at about 333 km s^{-1}; the R(1) line of CN appears at about 230 km s^{-1}. Note the velocity differences between the stronger component in Na I, CN, and CH (278 km s^{-1}), the weaker component in Na I and CH (267 km s^{-1}), and the stronger component in CH^+ (269 km s^{-1}).
(*right*) Four of the "C_2-DIBs" toward Sk−67°2 (*upper*) and toward ρ Oph A (*lower*). These weak, narrow DIBs, which are associated with enhanced C_2 and CN, are roughly half as strong toward Sk−67°2.

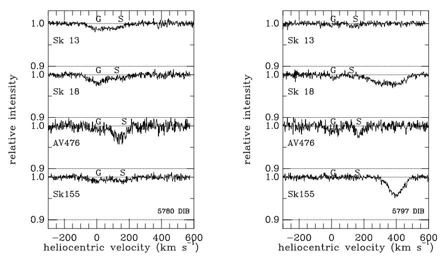

Figure 3. UVES spectra of DIBs at 5780 (*left*) and 5797 Å (*right*) toward 4 SMC stars. The vertical scale is expanded by a factor of 10. Letters G and S mark velocities of strongest Galactic and SMC Na I absorption; unmarked features red-ward of the 5797 Å DIB are stellar lines.

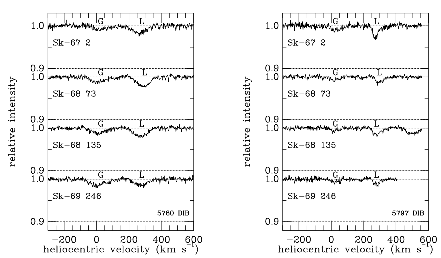

Figure 4. UVES spectra of DIBs at 5780 (*left*) and 5797 Å (*right*) toward 4 LMC stars. The vertical scale is expanded by a factor of 10. Letters G and L mark velocities of strongest Galactic and LMC Na I absorption; unmarked features red-ward of the 5797 Å DIB are stellar lines.

Molecular Lines

We now compare the column densities of several atomic and molecular species with each other and with the strengths of several of the diffuse interstellar bands. In each case, we first describe the general relationships found in the local Galactic ISM and in two more restricted regions ["Sco-Oph" and "Orion Trapezium" — where the behavior of Na I and K I differs somewhat from the general Galactic trends (e.g., Welty & Hobbs 2001)], then examine the corresponding relationships found for the SMC and LMC. Such comparisons, for the different environments probed in the three galaxies, may reveal useful diagnostics of the local physical conditions and may provide clues to the (still unknown) carriers of the DIBs. In many cases, the slope of the line fitted to the apparent "normal" Galactic relationship (Y vs. X) is close to either 1.0 or 0.5 — suggesting that Y is roughly proportional to either X or $(X)^{1/2}$.

The roughly linear relationship between the column densities of CH and H_2, found both for Galactic diffuse sightlines (Danks, Federman, & Lambert 1984) and for more reddened ("translucent") sightlines (e.g., Rachford et al. 2002), is displayed in Figure 5. This nearly linear relationship can be understood via models of gas-phase chemistry, in which the formation of CH is initiated by the reaction $C^+ + H_2$ and the destruction of CH is due primarily to photodissociation; the range in N(CH) at any given $N(H_2)$ may be due to differences in local density (Danks et al. 1984). The general Galactic relationship seems to hold as well for the seven Sco-Oph sightlines with detections of both H_2 and CH and for the six LMC sightlines (with the possible exception of that toward Sk−70°115). The two SMC sightlines with detections of H_2 and CH (Sk 18, AV476), however, have $N(CH)/N(H_2)$ ratios about an order of magnitude smaller than the Galactic average value, and the upper limit toward Sk 13 is a factor of 4 below that average value. Interestingly, the relative $N(CH)/N(H_2)$ ratios for the three galaxies (MW/LMC/SMC = 1.0/0.8/0.1) are not the same as the relative metallicities (1.0/0.5/0.2).

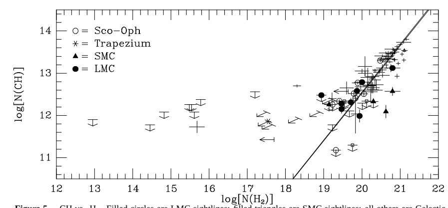

Figure 5. CH vs. H_2. Filled circles are LMC sightlines; filled triangles are SMC sightlines; all others are Galactic sightlines (open circles are Sco-Oph; open squares are Pleiades; asterisks are Orion Trapezium; open triangles are other "discrepant" sightlines). Solid lines show weighted and unweighted fits to the Galactic data (with slopes ∼ 1.1), for $N(H_2) \geq 10^{19}$ cm^{-2} and omitting various "discrepant" sightlines.

Welty & Hobbs (2001) noted both a fairly tight, nearly linear relationship between the column densities of CH and K I and striking similarities in the respective absorption-line profiles in a number of Galactic sightlines — suggestive of a generally close association between the two species. Figure 6 shows the relationships between N(CH) and the column densities of both K I and Na I (which is also tightly correlated with K I). In both cases, there is an essentially linear relationship between the two column densities (slopes ∼ 0.99–1.06), with very small rms scatter (≤ 0.15 dex) and very few "discrepant" points. The column density ratios log[N(CH)/N(K I)] and log[N(CH)/N(Na I)] for the Sco-Oph region (6–10 sightlines) and the LMC (4–7 sightlines) appear to be consistent with the overall Galactic values 1.30±0.20 and −0.65±0.19, respectively; the slightly lower than average N(Na I)/N(K I) ratios in those two regions are reflected in the slight differences from the average Galactic values. The average N(CH)/N(Na I) ratio for the two SMC sightlines with detections of both species is nearly a factor of 2 lower than the average Galactic ratio, but this difference is only marginally larger than the scatter in the Galactic values.

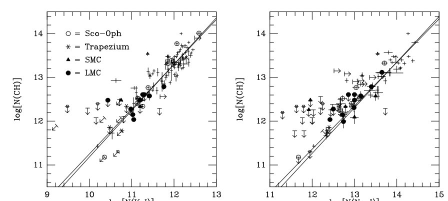

Figure 6. CH vs. K I (*left*) and CH vs. Na I (*right*). Filled circles are LMC sightlines; filled triangles are SMC sightlines; all others are Galactic sightlines (see caption to Fig. 5). Solid lines show weighted and unweighted fits to the Galactic data (with slopes ∼ 1.0; omitting "discrepant" sightlines).

Diffuse Interstellar Bands

Figure 7 shows the well-known Galactic correlations between the strengths of the 5780 Å DIB, the column density of H I, and the color excess $E(B-V)$ (e.g., Herbig 1995 and references therein; York et al. 2005); the 5797 Å and 6284 Å DIBs exhibit generally similar behavior (though with some differences). The slopes of the general Galactic relationships with both N(H I) and $E(B-V)$ are 1.0–1.3 for the 5780 and 5797 Å DIBs, and are 0.8–0.9 for the 6284 Å DIB; the rms scatter is ≤ 0.15 dex in all cases. Some regional differences are apparent, however, for the DIBs in the Galactic ISM. Toward the Sco-Oph stars, all three DIBs are weaker by a factor of about 2, relative to N(H I), but are consistent with the general trends versus $E(B-V)$. Toward the three Trapezium region stars, the three DIBs are weaker by factors of 3–10, relative to N(H I); the 5780 and 5797 Å DIBs are weaker by factors of about 2 and 4, respectively, relative to $E(B-V)$. The weakness of the DIBs versus N(H I) is reminiscent of the lower column densities of Na I and K I, for a given $N(H_{tot})$, noted for these two regions by Welty & Hobbs (2001). In the Magellanic Clouds, the three DIBs are (on average) even weaker — by factors of 7–9 (LMC) and factors of ∼ 15–20 (SMC), relative to N(H I), and by factors of about 2 (both LMC and SMC), relative to $E(B-V)$; N(Na I) and N(K I) are also much lower in the LMC and SMC, for a given $N(H_{tot})$, than in the local Galactic ISM (Welty 2005). These differences are reasonably consistent with the differences in metallicity, dust-to-gas ratio, and interstellar radiation field among the three galaxies, if the field is typically ∼ 5 times stronger in the LMC and SMC (Lequeux 1989).

Figure 7 — and similar figures for the 5797 and 6284 Å DIBs — indicate that the strengths of the three DIBs also appear to be correlated with the column densities of both Na I and K I (e.g., Herbig 1993), though with somewhat larger rms scatter (0.15–0.26 dex) and correspondingly smaller correlation coefficients than those characterizing the relationships with N(H I) and $E(B-V)$. The slopes of the general Galactic relationships with N(Na I) and N(K I), however, are smaller — 0.5–0.7 for the 5780 and 5797 Å DIBs and 0.3–0.4 for the 6284 Å DIB — suggesting that the DIB strengths may be roughly proportional to the square roots of the column densities of the two trace neutral species. There are also some apparent regional differences in average DIB strength versus both $[N(\text{Na I})]^{1/2}$ and $[N(\text{K I})]^{1/2}$. Toward the Sco-Oph stars, the three DIBs are consistent with the general Galactic values, relative to $[N(\text{K I})]^{1/2}$, but are stronger by a factor of about 2, relative to $[N(\text{Na I})]^{1/2}$ — due, presumably, to the slight relative weakness of Na I in that region. Toward the Trapezium stars, the strength of the 5797 Å DIB, relative to both $[N(\text{K I})]^{1/2}$ and $[N(\text{Na I})]^{1/2}$, is consistent with the general Galactic values, but the corresponding ratios for the 5780 and 6284 Å DIBs are factors of about 2 and 4 higher, respectively. In both the LMC and SMC, the three DIBs are all weaker, by average factors of about 1.5 and 3, relative to $[N(\text{Na I})]^{1/2}$ and $[N(\text{K I})]^{1/2}$, respectively. There are, however, individual sightlines in the LMC and SMC for which some of the ratios may be consistent with typical Galactic values.

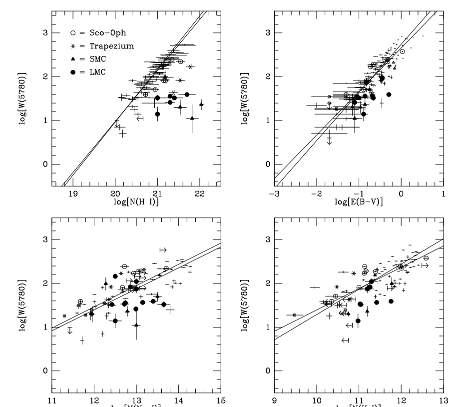

Figure 7. 5780 Å DIB vs. N(H I) (*upper left*), vs. $E(B-V)$ (*upper right*), vs. N(Na I) (*lower left*), and vs. N(K I) (*lower right*). Filled circles are LMC sightlines; filled triangles are SMC sightlines; all others are Galactic sightlines (see caption to Fig. 5). Solid lines show weighted and unweighted fits to the Galactic data (with slopes ∼ 1.0–1.2 for H I and $E(B-V)$ and ∼ 0.5 for Na I and K I; omitting "discrepant" sightlines).

Summary / Conclusions

- CH and/or CH^+ are detected in the LMC toward 8 stars and in the SMC toward 2 stars; CN is detected in the LMC toward 1 star.
- The average $N(CH)/N(H_2)$ ratios in the Milky Way, LMC, and SMC go as 1.0/0.8/0.1 — somewhat different from the relative metallicities (1.0/0.5/0.2).
- On average, the LMC and SMC DIBs at 5780, 5797, and 6284 Å are factors of ∼ 7–20 weaker, relative to H I, and are factors of ∼ 1.5–3.0 weaker, relative to $E(B-V)$, Na I, K I, than in our Galaxy — consistent with the differences in metallicity, dust-to-gas ratio, and radiation field.
- Such comparisons may provide clues to the identity of the DIB carrier(s) and may also yield diagnostics for the shape and strength of the radiation field.

REFERENCES

Danks, A. C., Federman, S. R., & Lambert, D. L. 1984, A&A, 130, 62
Ehrenfreund, P., Cami, J., Jimenez-Vicente, J. et al. 2002, ApJ, 576, L117
Herbig, G. H. 1993, ApJ, 407, 142
Herbig, G. H. 1995, ARA&A, 33, 19
Lequeux, J. 1989, in Recent Developments of Magellanic Cloud Research (Paris Obs.)
Magain, P., & Gillet, D. 1987, A&A, 184, L5
Pak, S., Jaffe, D. T., van Dishoeck, E. F., Johansson, L. E. B., & Booth, R. S. 1998, ApJ, 498, 735
Rachford, B., Snow, T. P., Tumlinson, J. et al. 2002, ApJ, 577, 221
Thorburn, J. A., Hobbs, L. M., McCall, B. J. et al. 2003, ApJ, 584, 339
Tumlinson, J., Shull, J. M., Rachford, B. L. et al. 2002, ApJ, 566, 857
Vidal-Madjar, A., Andreani, P., Cristiani, S., Ferlet, R., Lanz, T., & Vladilo, G. 1987, A&A, 177, L17
Welty, D. E. 2005, in preparation
Wolfire, M. G., Hollenbach, D. J., McKee, C. F., Tielens, A. G. G. M., & Bakes, E. L. O. 1995, ApJ, 443, 152
York, D. G. et al. 2005, in preparation

This miniposter was prepared with Brian Wolven's Poster LaTeX macros v2.1.

We thank P. Crowther for contributing UVES spectra of several LMC stars. Support has been provided by NASA LTSA grant NAG5-11413 to the University of Chicago.